Heat Transport in Turbulent Rayleigh-Bénard Convection

Xiaochao Xu, Kapil M. S. Bajaj, and Guenter Ahlers

Department of Physics and Quantum Institute, University of California, Santa Barbara, California 93106
(Received 19 January 2000)

We present measurements of the Nusselt number $\mathcal{N}$ as a function of the Rayleigh number R in cylindrical cells with aspect ratios $0.5 \leq \Gamma \equiv D/d \leq 12.8$ (D is the diameter and d is the height). We used acetone with a Prandtl number $\sigma = 4.0$ for $10^5 \lesssim R \lesssim 4 \times 10^{10}$. A fit of a power law $\mathcal{N} = \mathcal{N}_0 R^{\gamma_{\text{eff}}}$ over limited ranges of R yielded values of γ_{eff} from 0.275 near $R = 10^7$ to 0.300 near $R = 10^{10}$. The data are inconsistent with a single power law for $\mathcal{N}(R)$. For $R > 10^7$ they are consistent with $\mathcal{N} = a\sigma^{-1/12}R^{1/4} + b\sigma^{-1/7}R^{3/7}$ as proposed by Grossmann and Lohse for $\sigma \gtrsim 2$.

Since the pioneering measurements by Libchaber and co-workers [1,2] of heat transport by turbulent gaseous helium heated from below, there has been a revival of interest in the nature of turbulent convection [3]. In addition to the local properties of the flow, one of the central issues has been the global heat transport of the system, as expressed by the Nusselt number $\mathcal{N} = \lambda_{\text{eff}}/\lambda$. Here $\lambda_{\text{eff}} = qd/\Delta T$ is the effective thermal conductivity of the convecting fluid (q is the heat-current density, d is the height of the sample, and ΔT is the imposed temperature difference), and λ is the conductivity of the quiescent fluid. Usually a simple power law

$$\mathcal{N} = \mathcal{N}_0 R^{\bar{\gamma}} \qquad (1)$$

was an adequate representation of the experimental data within their resolution of a percent or so [4]. Here $R = \alpha g d^3 \Delta T/\kappa\nu$ is the Rayleigh number, α is the thermal expansion coefficient, g is the gravitational acceleration, κ is the thermal diffusivity, and ν is the kinematic viscosity. Various data sets yielded exponent values $\bar{\gamma}$ from 0.28 to 0.31 [5,6]. Most recently, measurements over the unprecedented range $10^6 \lesssim R \lesssim 10^{17}$ were made by Niemela *et al.,* and a fit to them of Eq. (1) gave $\bar{\gamma} = 0.309$ [5], but even over this extremely wide range these data did not have the resolution to reveal deviations from the functional form of Eq. (1). Competing theoretical models also made predictions of power-law behavior, with γ in the same narrow range [2,6–8]. For example, a boundary-layer scaling theory [2,8] which yielded $\gamma = 2/7 \simeq 0.2857$ was an early favorite, at least for the experimentally accessible range $R \lesssim 10^{12}$. It was generally consistent with most of the available experimental results. However, very recently a competing model based on the decomposition of the kinetic and the thermal dissipation into boundary-layer and bulk contributions was presented by Grossmann and Lohse (GL) [7] and predicted non-power-law behavior. According to GL, the data measure an average exponent $\bar{\gamma}$ associated with a crossover from $\gamma = 1/4$ at small R to a slightly larger γ at much larger R. In the experimental range the effective exponent $\gamma_{\text{eff}} \equiv d[\ln(\mathcal{N})]/d[\ln(R)]$, which should be compared with the experimentally determined $\bar{\gamma}$, is close to $2/7$ and depends only weakly upon R.

Within the typical experimental resolution of a percent or so, it has not been possible before to distinguish between these competing theories.

Here we present new measurements of $\mathcal{N}(R)$ over the range $10^5 \lesssim R \lesssim 4 \times 10^{10}$ for a Prandtl number $\sigma \equiv \nu/\kappa = 4.0$. Our data are of exceptionally high precision and accuracy. They are incompatible with the single power law equation (1), and yield values of γ_{eff} which vary from 0.277 near $R = 10^7$ to 0.300 near $R = 10^{10}$. In particular, the results rule out the prediction [2,8] $\gamma = 2/7$. For $R \gtrsim 10^7$ a much better fit to our results can be obtained with the crossover function,

$$\mathcal{N} = a\sigma^{-1/12}R^{1/4} + b\sigma^{-1/7}R^{3/7}, \qquad (2)$$

proposed by GL [7] for $\sigma \gtrsim 2$.

We used two apparatus. One was described previously [9]. It could accommodate cells with a height up to $d = 3$ cm. The other was similar, except that its three concentric sections were lengthened by 20 cm to allow measurements with cells as long as 23 cm. In both, the cell top was a sapphire disk of diameter 10 cm. A high-density polyethylene sidewall of circular cross section and with diameter D close to 8.8 cm was sealed to the top and bottom by ethylene-propylene O rings. Four walls, with heights ranging from 0.70 to 17.4 cm, were used and yielded aspect ratios $\Gamma \equiv D/d = 12.8, 2.0, 1.0,$ and 0.5. The bottom plate had a mirror finish and contained two thermistors. The fluid was acetone [10]. From Eq. (8) of Ref. [11], we estimated $x \simeq 1 + 0.0012\Delta T$ for the ratio of the temperature drops across the top and bottom boundary layers. Our temperature stability and resolution was 0.001 °C or better. We measured and corrected for the conductances of the empty cells, and applied corrections for resistance in series with the fluid. The bath and bottom-plate temperatures usually fluctuated by no more than a few mK. Usually ΔT was stepped in equal increments on a logarithmic scale, holding the mean temperature close to 32.00 °C.

Results of our measurements in four cells of different Γ are shown in Fig. 1. For each cell they cover about two decades of R, and collectively they span the range of R from 10^5 to 4×10^{10}. There is a dependence of $\mathcal{N}(R)$
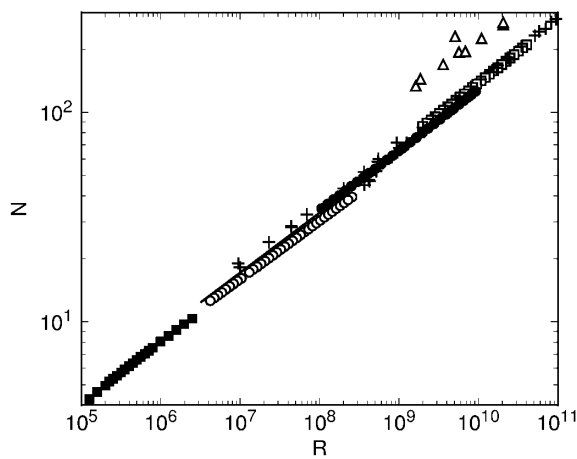
FIG. 1. The Nusselt number as a function of the Rayleigh number. Solid squares: $\Gamma = 12.8$; open circles: $\Gamma = 3.0$; solid circles: $\Gamma = 1.0$; open squares: $\Gamma = 0.50$; plusses: Ref. [13]; open triangles: Ref. [14]; solid line: Ref. [15].

upon Γ, as already noted by others [12]. For comparison, we also show in Fig. 1 the recent results of Chavanne *et al.* [13] for $\sigma \simeq 0.8$ and $\Gamma = 0.5$ (plusses) and those of Ashkenazi and Steinberg [14] for $\sigma = 1$ and a cell of square cross section and $\Gamma = 0.72$ (open triangles). There is good agreement with the former, considering the difference in σ. The latter are about a factor of 1.6 larger than our results; this difference seems too large to be attributed to the difference in σ or the geometry and remains unexplained. The solid line just above the open circles in the figure (more easily seen in Fig. 2) corresponds to the fit of Eq. (1) to the data of Liu and Ecke [15] for $\sigma = 4$, $\Gamma \simeq 1$, and a cell with a square cross section. The agreement with our data is excellent, considering the difference in geometry.

Figure 1 does not have enough resolution to reveal details about the data. Thus we use the early prediction $\gamma = 2/7$ as a reference, and show $\log_{10}(\mathcal{N}R^{-2/7})$ as a function of $\log_{10}(R)$ in Fig. 2. If the theory were correct,
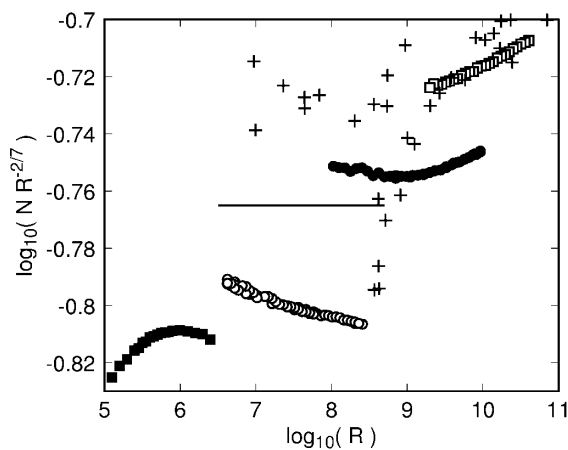
$\mathcal{N}R^{-2/7}$ should be equal to $\mathcal{N}_0$, i.e., independent of R. If Eq. (1) is the right functional form but γ differs from $2/7$, then the data should fall on straight lines with slopes equal to $\gamma - 2/7$. Our $\Gamma = 12.8$ data (solid squares) are at relatively small R and one might not expect Eq. (1) to become applicable until R is larger. The $\Gamma = 3.0$ data actually show slight curvature, but in any case would yield $\bar{\gamma} < 2/7$. The smaller-Γ data are clearly curved, showing that Eq. (1) is not applicable with any value of γ. In order to make this conclusion more quantitative, we show in Fig. 3 effective local exponents γ_{eff} derived by fitting Eq. (1) to the data over various restricted ranges, each covering about half a decade of R. The fits yield values of $\gamma_{\text{eff}}(R)$ which have a minimum near $R = 10^7$. Within our resolution γ_{eff} is independent of Γ.

To the extent that γ_{eff} does not depend upon Γ, it is possible to write $\mathcal{N}(R, \Gamma)$ as

$$\mathcal{N}(R, \Gamma) = f(\Gamma)F(R), \tag{3}$$

in terms of a scale factor $f(\Gamma) = \mathcal{O}(1)$ and a scaling function $F(R)$ which is independent of Γ. In Fig. 4 we show $\log_{10}[R^{-2/7}F(R)]$ as a function of $\log_{10}(R)$. Here we chose arbitrarily the $\Gamma = 1$ data as a reference and assigned them the value $f(\Gamma = 1) = 1$. One sees that the data for all Γ collapse onto a universal curve.

Next we compare the predictions of GL [7] with our data. These authors defined various scaling regimes in the $R - \sigma$ plane. For $\sigma \gtrsim 2$, they expect that crossover between their regions I_u and III_u should be observed. For that case, Eq. (2) is predicted to apply. One way to test this [16] is to plot $y = [\mathcal{N}/f(\Gamma)]/(R^{1/4}\sigma^{-1/12})$ as a function of $x = R^{5/28}\sigma^{-5/84}$. If the prediction is correct, the data should fall on a straight line $y = a + bx$ with a and b equal to the coefficients in Eq. (2). Our data are shown in this parametrization in Fig. 5. The solid line is a least-squares fit to the $\Gamma = 1$ data. The fit is extremely good. The coefficients are $a = 0.326$ and $b = 2.36 \times 10^{-3}$, in good agreement with the coefficients
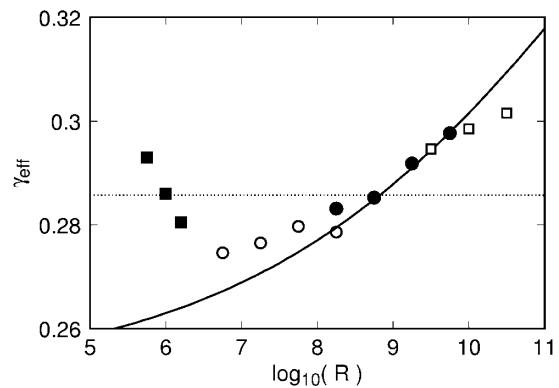

FIG. 2. High-resolution plot of the Nusselt number as a function of the Rayleigh number. The symbols are as in Fig. 1.

FIG. 3. The effective exponent as a function of R. Solid squares: $\Gamma = 12.8$. Open circles: $\Gamma = 3.0$. Solid circles: $\Gamma = 1.0$. Open squares: $\Gamma = 0.5$. Solid line: logarithmic derivative of Eq. (2) with $a = 0.326$ and $b = 2.36 \times 10^{-3}$. Dotted line: $\gamma = 2/7$.
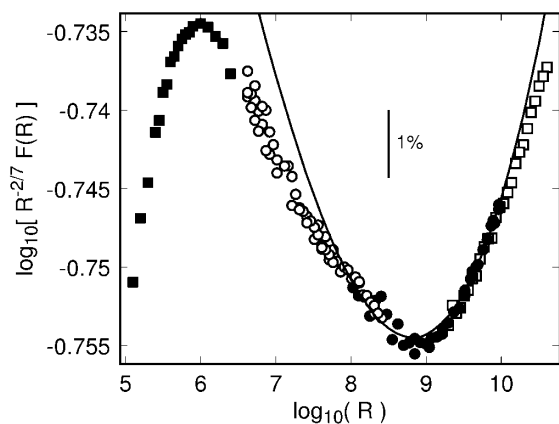
FIG. 4.   High-resolution plot of the scaling function $F(R)$ defined by Eq. (3). The symbols are as in Fig. 1. We used the scale factors $f(\Gamma) = 0.933, 1.000, 1.131$, and 1.186 for $\Gamma = 0.5, 1.0, 3.0$, and 12, respectively. The solid line corresponds to a fit of the prediction of GL to the $\Gamma = 1$ data.

estimated by GL on the basis of other experiments [17]. At small R the $\Gamma = 3$ data deviate slightly from the GL prediction. This may be because the values of R are too small for the GL function to apply. GL estimate that their region I_u has a lower boundary below which the Reynolds number of a large-scale flow, which they predict to be given by $R_e \simeq 0.039 R^{1/2} \sigma^{-5/6}$, is less than about 50. This occurs when $R \simeq 1.6 \times 10^7$, corresponding to $R^{5/28} \sigma^{-5/84} = 17.8$. This value is indicated in Fig. 5 by the small vertical bar.

At large R the $\Gamma = 0.5$ data also deviate slightly from the GL fit to the $\Gamma = 1$ data. However, we feel that these deviations are so small that one cannot assert that they exceed possible systematic errors. In the range of R where they occur, the temperature differences are already quite large, and small effects due to deviations from the Boussinesq approximation cannot at present be ruled out.

It would be desirable to make measurements in a much larger cell where these Rayleigh numbers could be reached with more modest temperature differences.

Finally, we note that small deviations from the GL prediction Eq. (2) might occur because σ is not sufficiently much larger than the crossover value $\sigma \simeq 2$ above which Eq. (2) is applicable. It would be desirable to determine $F(R)$ using other fluids which have larger Prandtl numbers. However, for these fluids larger cells will be required in order to reach the same maximum R.

The logarithmic derivative γ_{eff} of Eq. (2) based on the parameters a and b determined from the fit to the $\Gamma = 1$ data is shown as a solid line in Fig. 3. For $R \gtrsim 10^7$ the line agrees quite well with the values determined by local fits of Eq. (1) to the data. The small, seemingly systematic, deviations which do exist at large and small R correspond to the deviations from the straight line in Fig. 5 and were discussed above for that parametrization.

Finally, we ask whether the agreement between the theory and the data is sensitive to the details of the GL prediction. For large σ, the theory predicts crossover from I_u to III_u and Eq. (2) [7]. For somewhat smaller $\sigma \simeq 1$, however, the crossover should be from I_u to IV_u, and the prediction then reads [7]

$$\mathcal{N} = a\sigma^{-1/12}R^{1/4} + bR^{1/3}. \qquad (4)$$

As a function of σ, GL estimate that the transition from Eq. (2) to Eq. (4) occurs near $\sigma = 2$, but there is some uncertainty in this value. Thus, in Fig. 6 we compared Eq. (4) with our results for $\Gamma = 1$ by plotting $y = \mathcal{N}/(R^{1/4}\sigma^{-1/12})$ as a function of $x = R^{1/12}\sigma^{1/12}$. If Eq. (4) is applicable, this should yield a straight line. As can be seen, the data deviate systematically from the fit. Thus a transition from I_u to IV_u at $\sigma = 4$ is inconsistent with our data.

In Fig. 7 we show the deviations $\delta\mathcal{N}/\mathcal{N}$ from fits of Eqs. (1), (2), and (4) to the $\Gamma = 1.0$ data. For Eq. (1) they
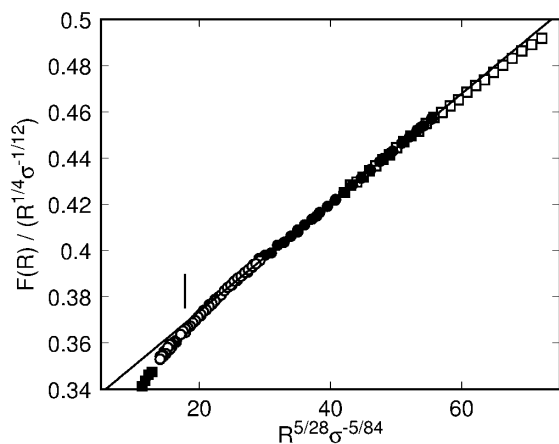

FIG. 5.   Plot of $F(R)/(R^{1/4}\sigma^{-1/12})$ as a function of $R^{5/28}\sigma^{-5/84}$. The symbols are as in Fig. 1. The straight line is a least-squares fit to the $\Gamma = 1$ data. The small vertical bar indicates an estimate of the lower limit of applicability of the GL prediction.
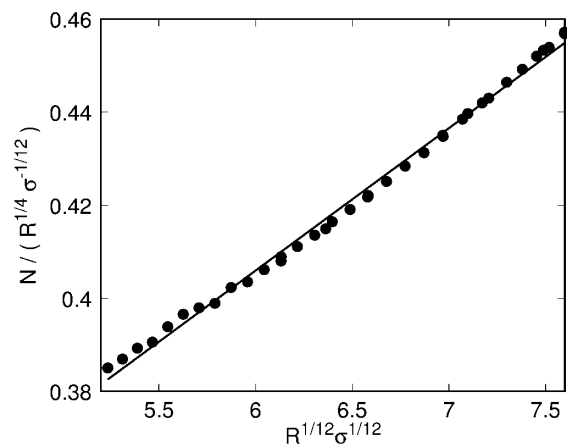

FIG. 6.   Plot of $\mathcal{N}/(R^{1/4}\sigma^{-1/12})$ as a function of $R^{1/12}\sigma^{1/12}$. If Eq. (4) is correct, the points should fall on the straight line, a least-squares fit. The data deviate systematically, showing that Eq. (4) is not the right functional form.
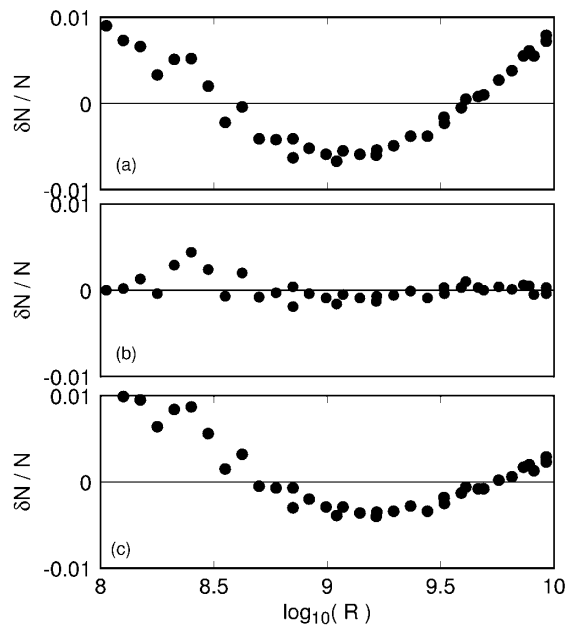
FIG. 7. Relative deviations $\delta\mathcal{N}/\mathcal{N}$ from fits of (a) Eq. (1), (b) Eq. (2), and (c) Eq. (4) to the $\Gamma = 1.0$ data.

are systematic, as already expected. For Eq. (2) the fit is nearly perfect. For Eq. (4) the deviations are nearly as large as those for Eq. (1). Thus Eq. (4) is not applicable to the data, and of the three functional forms which we examined only Eq. (2) provides a satisfactory fit.

All of the work reported here has concentrated on measurements of $\mathcal{N}(R)$ for acetone with $\sigma = 4.0$. We conclude that there is no significant range of R over which the power law equation (1) is applicable, and that the crossover function equation (2) proposed by Grossmann and Lohse provides a good fit to the data for $R \gtrsim 10^7$ where the Reynolds number of the large-scale flow is expected [7] to exceed about 50. Obviously a great deal of additional high-precision work remains to be done. An apparatus with a larger cell, with $d \simeq 50$ cm, for instance, could be constructed and would permit measurements with acetone up to $R \simeq 10^{12}$. To provide further tests of the GL predictions, a systematic study of $\mathcal{N}(R,\sigma)$ as a function of σ should be carried out. This can be done using various fluids such as methanol, ethanol, and 2-propanol. Since the Reynolds number is central to the GL theory, its determination is also an obvious area for further work. And finally, measurements of comparable accuracy and precision should be extended to the compressed gases where $\sigma \simeq 0.7$, where more direct comparison with much previous work [3,6] is possible, and where a different GL crossover function [7] should pertain.

[1] F. Heslot, B. Castaing, and A. Libchaber, Phys. Rev. A **36**, 5870 (1987).

[2] B. Castaing, G. Gunaratne, F. Heslot, L. Kadanoff, A. Libchaber, S. Thomae, X. Z. Wu, S. Zaleski, and G. Zanetti, J. Fluid Mech. **204**, 1 (1989).

[3] For reviews, see E. D. Siggia, Annu. Rev. Fluid Mech. **26**, 137 (1994); S. Zaleski, in *Geophysical and Astrophysical Convection,* edited by P. Fox and R. Kerr (Gordon and Breach, New York, 1998).

[4] Data taken with helium gas by Chavanne *et al.* [X. Chavanne, F. Chilla, B. Chabaud, B. Castaing, J. Chaussy, and B. Hébral, J. Low Temp. Phys. **104**, 109 (1996)] show a departure from a power law with $\gamma = 2/7$ for $R > 3 \times 10^{10}$. However, these results differ from those of Niemela *et al.* [5], which were also obtained with helium gas. The results of Cioni *et al.* [S. Cioni, S. Ciliberto, and J. Sommeria, J. Fluid Mech. **335**, 111 (1997)] for liquid mercury also suggest a deviation from Eq. (1), but these results are for the very different Prandtl number regime $\sigma \simeq 0.025$.

[5] J. J. Niemela, L. Skrbek, K. R. Sreenivasan, and R. J. Donnelly, Nature (to be published).

[6] A detailed examination of the recent experimental and theoretical literature was presented recently in Ref. [7].

[7] S. Grossmann and D. Lohse, J. Fluid Mech. **407**, 27 (2000).

[8] B. I. Shraiman and E. D. Siggia, Phys. Rev. A **42**, 3650 (1990).

[9] M. A. Dominguez-Lerma, G. Ahlers, and D. S. Cannell, Phys. Rev. E **52**, 6159 (1995).

[10] See T. E. Daubert and R. P. Danner, *Physical and Thermodynamic Properties of Pure Chemicals* (Hemisphere Publishing Corporation, New York, 1989) for properties of organic fluids.

[11] X.-Z. Wu and A. Libchaber, Phys. Rev. A **43**, 2833 (1991).

[12] X.-Z. Wu and A. Libchaber, Phys. Rev. A **45**, 842 (1992).

[13] X. Chavanne *et al.,* in Ref. [4].

[14] S. Ashkenazi and V. Steinberg, Phys. Rev. Lett. **83**, 3641 (1999).

[15] Y. Liu and R. E. Ecke, Phys. Rev. Lett. **79**, 2257 (1997).

[16] We are grateful to Detlef Lohse for suggesting this graphical representation.

[17] It was assumed that $\mathcal{N}$ is the appropriate variable to compare with Eqs. (1) and (2). One might argue that only the convective contribution $\mathcal{N} - 1$ should be considered. Replacing $\mathcal{N}$ with $\mathcal{N} - 1$ leads to similar conclusions.